PARAMETER OPTIMIZATION AND EXPERIMENT OF A SINGLE LONGITUDINAL AXIAL FLOW FULL-CIRCUMFERENCE SEPARATION THRESHING DEVICE FOR RAPESEED HARVESTER

/

油菜收割机单纵轴流全周分离脱粒装置参数优化与试验

Min ZHANG, Chenke XU, Chengpeng LI, Gang WANG, Yao YANG, Tao JIANG
Nanjing Institute of Agricultural Mechanization, Ministry of Agriculture and Rural Affairs of China, Nanjing 210014, China
Tel: +86.15366092917; E-mail: zhm0912@126.com
DOI: https://doi.org/10.35633/inmateh-76-103

Keywords: *rapeseed, combine harvester, threshing device, EDEM, parameter optimization*

ABSTRACT

A discrete element model (DEM) of rapeseed threshing and separation was established based on EDEM software. The simulation results were compared with bench test data, showing an absolute error of 0.33% and a relative error of 55% for threshing loss. The relative errors for the proportion of threshed material on the sieve surface and the left–right distribution ratio of threshed material on the sieve surface were 1.21% and 2.38%, respectively, verifying the accuracy of the simulation model. Secondly, a three-factor, three-level Box–Behnken experimental design was conducted, with threshing drum speed, guide plate angle, and threshing gap as test factors, and threshing loss, proportion of threshed material on the sieve surface, and left–right distribution ratio of the threshed material as evaluation indicators. The influence of each factor on the evaluation indicators was analyzed, and regression models between the test factors and evaluation indicators were established. Through a multi-objective optimization solution, combined with consideration of the actual operating conditions and processing requirements of the rapeseed combine harvester, the optimal parameter combination was determined as: drum speed of 550 r/min, guide plate angle of 75°, and threshing gap of 8 mm. Finally, a prototype was developed based on the optimized structure and operating parameters, and its rapeseed harvesting performance was tested by a third-party inspection agency. Field tests showed a total harvest loss rate of 5.6%, impurity rate of 2.3%, breakage rate of 0.4%, and an operational productivity of 0.57 hm²/h. The performance exceeded the requirements of industry standards. This study provides a valuable reference for the performance optimization of threshing devices.

摘要

基于 EDEM 软件构建了油菜脱粒分离离散元模型，仿真结果和台架对比试验表明，脱粒损失绝对误差为 0.33%，相对误差为 55%，筛面脱出物占比和筛面脱出物左右比值的相对误差分别为 1.21%和 2.38%，验证了仿真模型的准确新。以脱粒滚筒转速、导草板角度和脱粒间隙为试验因素，以脱粒损失、筛面脱出物占比和筛面脱出物左右分布比值为评价指标，开展了三因素三水平 Box-Behnken 试验，分析了各因素对评价指标的影响关系，建立了试验因素与评价指标之间的回归数学模型，通过多目标优化求解，结合油菜联合收割机实际工况和加工要求，确定优化后的参参数组合为：滚筒转速 550 r/min，导草板角度 75°，脱粒间隙 8 mm。在最优结构和工作参数下，试制了样机并委托第三方检测机构对油菜收获作业性能进行了检测，田间实测收获总损失率 5.6%、含杂率 2.3%、破碎率 0.4%，作业小时生产率 0.57hm²/h，作业性能优于行业标准要求。该研究可为脱粒装置性能优化提供参考。

INTRODUCTION

The threshing device is the core working component of a rapeseed combine harvester. Based on its configuration, it can be categorized into transverse axial–flow and longitudinal axial-flow types. When the device is arranged transversely, the threshing and separation capacity is limited by the horizontal length of the threshing drum. In contrast, a longitudinal configuration allows for unrestricted drum length, offering advantages such as higher efficiency and better economic performance (*Yang et al., 2018; Tang et al., 2013*). However, longitudinal axial-flow threshing devices also face challenges such as excessive stalk breakage due to delayed separation of threshed material, a high proportion of threshed material that increases the cleaning load, and low utilization of the sieve surface.

To enhance the processing capacity and cleaning efficiency of threshing devices, internationally renowned combine harvester manufacturers such as John Deere, CLAAS, and Geringhoff have developed advanced threshing systems, including tangential–axial flow combination types and dual axial-flow threshing and separation drums. These multi-drum configurations increase the threshing path and separation area, improving material throughput and screen penetration (*Dong et al., 2023; Teng et al., 2020; Mirzazadeh et al. 2012; Yuan et al., 2024*). Additionally, features such as segmented sieve boxes, material guide plates, and intelligent control technologies that adjust the vibration state of the cleaning sieve help achieve more uniform material distribution on the sieve surface, thereby improving post-threshing cleaning performance. However, these systems also present challenges, including structural complexity and large overall geometry, making them suitable only for large scale harvesters (*Xu et al., 2011; Qian et al., 2017; Yang et al., 2010*). Miu et al. developed a variable diameter threshing device that adjusts the threshing gap by changing the drum diameter during operation. This allows for the regulation of threshing intensity at different stages, thereby reducing grain damage and breakage of threshed material (*Miu et al., 2007; Wang et al., 2020; Trollope et al., 1982; Tang et al., 2012*). *Xu et al.* (*2020*) designed a combined tangential–axial flow double-drum threshing device for rapeseed, where easily threshed parts undergo preliminary threshing, and the more difficult parts enter a longitudinal axial-flow threshing drum (*Xu et al., 2014; Wu et al., 2024; Fang et al., 2024)*. This design reduces threshing damage, decreases the frequency of threshed material impact, and improves both threshing and cleaning efficiency. The above studies indicate that increasing the separation area of the threshing device, accelerating the separation of threshed material *(Fu et al., 2024; Yang et al., 2024; Dai et al., 2022; Jiang et al., 2023)*, reducing the frequency of threshed material impact, and minimizing material fragmentation and the proportion of threshed material can not only enhance the performance of the threshing device but also contribute to improving the cleaning efficiency in the subsequent cleaning process.

Our team previously designed a single longitudinal axial–flow full–circle separation threshing device for rapeseed harvesting by increasing the separation area of the threshing device and employing a concave screen that rotates counter to the threshing drum to enhance rubbing and reduce material impact intensity. Preliminary tests were conducted using evaluation indicators such as the left–right distribution of threshed material on the sieve surface and the left–right distribution ratio of threshed material. Key parameters such as drum speed, guide plate angle, and threshing gap were analyzed to identify the main factors affecting threshing and separation performance and to determine the optimal parameter combination, and experimental verification was carried out.

MATERIALS AND METHODS

STRUCTURE AND WORKING PRINCIPLE OF THE THRESHING DEVICE

The structure of the single longitudinal axial-flow full-circle separation threshing device for rapeseed combine harvesters is shown in Figure 1. It mainly consists of a spiral conveyor, a rasp bar–spike tooth threshing drum, a full-circle separation concave screen, a guide plate, and a transmission system. The threshing drum rotates driven by the main engine of the combine harvester, while the concave screen is driven by the sprocket reducer to rotate in the opposite direction relative to the threshing drum. The working principle of this threshing device is as follows: material is fed into the threshing device by the spiral conveyor. Through the rotation of the threshing drum and the reverse rotation of the concave screen, the rapeseed material is subjected to impact and rubbing actions from the threshing components. This causes stalks to break and the grains to separate from the pod shells. Short stalks, residues, and grains pass through the concave screen and fall downward, while long stalks and large impurities are discharged from the rear end of the threshing device.

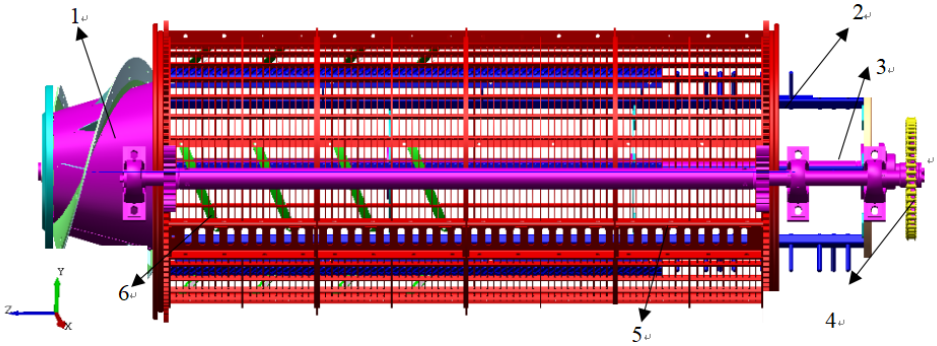

Fig. 1 - Single Longitudinal Axial-Flow Full-Circle Separation Threshing Device

1. Spiral Conveyor; 2. Rasp Bar–Spike Tooth Threshing Drum; 3. Sprocket Transmission System; 4. Full-Circle Concave Screen; 5. Guide Plate

Threshing gap, guide plate angle, and the rotational speeds of the threshing drum and concave screen are the core structural parameters of this threshing device. The threshing drum is designed with a diameter of 628 mm and a length of 1770 mm. The concave screen has a diameter of 705 mm and a length of 1542 mm. The spike teeth are 115 mm in height, with a total of 30 teeth. The rasp bars are 1240 mm long, with six bars in total. The threshing drum has six rod teeth, with the rasp bars and spike teeth evenly distributed across these six rods.

SIMULATION ANALYSIS OF THE THRESHING AND SEPARATION PROCESS

The discrete element method (DEM) was used to conduct simulation analysis in order to analyze the threshing and separation performance of the single longitudinal axial-flow full-circle separation threshing device, aiming to determine the optimal combination of structural parameters for the threshing device.

DISCRETE ELEMENT MODEL OF THE THRESHING DEVICE

Using the EDEM discrete element method, the material flow distribution during the rapeseed threshing process was analyzed. The single longitudinal axial–flow full–circle separation threshing device was modeled and simplified in the 3D modeling software SolidWorks, and components such as bearings and sprockets that did do not affect the simulation results were removed. Receiving boxes were placed below and behind the threshing system to collect and quantify the mass and composition of the material falling into each collection area. The components were grouped into five parts: the housing cover, threshing drum, counter-rotating concave screen, receiving box, and particle factory. The Hertz–Mindlin contact model was selected for the simulation. Both the threshing drum and concave screen were set to rotational motion and remained in continuous motion throughout the entire simulation, as shown in Figure 2.

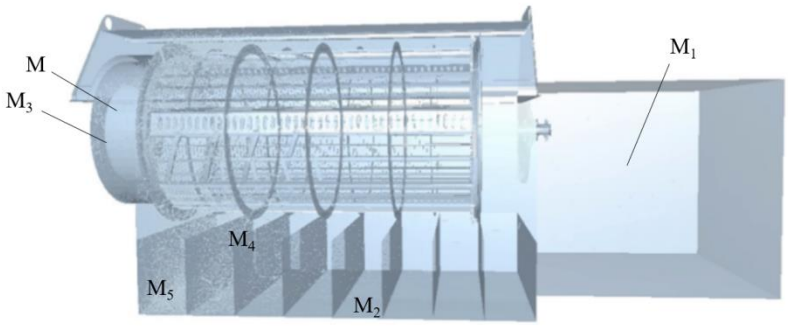

Fig. 2 - Simplified Model of the Threshing Device

DETERMINATION OF SIMULATION PARAMETERS

The collision and movement of rapeseed threshed material within the threshing device are complex. This study employs a soft-particle contact model, which simplifies the normal forces between particles into springs and dampers, and the tangential forces into springs, dampers, and sliders. In the soft–sphere contact model, the elastic and damping coefficients are determined based on Hertz contact theory. The threshed material in the threshing device consists of three components: grains, pods, and stalks. Taking the rapeseed variety Qinyou No. 10 as the research object and based on field preliminary experiments, the rapeseed grain model is simplified as a sphere with a diameter of 2 mm. The short stalks are simplified as cylinders with a diameter of 10 mm, which were randomly generated between 50.4-84 mm in length. The pods are randomly generated between 35-50 mm in length. A schematic diagram of the simplified rapeseed material model is shown in Figure 3.

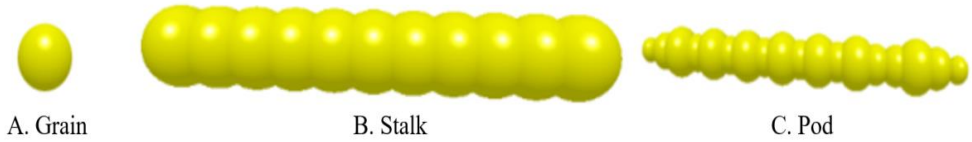

Fig. 3 - Schematic Diagram of the Simplified Threshed Material Model

This study primarily focuses on the distribution patterns of threshed material during rapeseed combined harvesting. The threshing device is made of 45# steel, and the simulation uses the previously determined basic Hertz–Mindlin particle model parameters. The material properties and contact simulation parameters between materials are listed in Tables 1 and 2.

A cylindrical virtual particle factory is set up around the spiral feeding inlet to generate material particles. The particle factory type is set to dynamic, and the material generation mode is configured as Total Mass.

Table 1

Simulation Parameters of the Material

Material Name	Poisson's Ratio	Density (kg/m^3)	Shear Modulus (MPa)
Grain	0.30	1069	7
Pod	0.33	894	1.8
Stalk	0.38	586	66.69
Threshing Device	0.30	7850	70000

Table 2

Contact Parameters Between Materials

Name	Restitution Coefficient	Static Friction Coefficient	Rolling Friction Coefficient
Grain–Grain	0.41	0.52	0.01
Grain–Pod	0.30	0.45	0.01
Grain–Stalk	0.33	0.35	0.01
Grain–Threshing Device	0.50	0.30	0.01
Pod–Pod	0.3	0.35	0.01
Pod–Stalk	0.35	0.33	0.01
Pod–Threshing Device	0.35	0.45	0.01
Stalk–Stalk	0.42	0.31	0.01
Stalk–Threshing Device	0.35	0.40	0.01

PERFORMANCE EVALUATION INDICATORS OF THE THRESHING DEVICE

(1) Threshing Loss Rate

In the EDEM post-processing, a material box with a Grid Bin Group of 1×1×1 is set up at the rear end of the threshing device to collect and count the grains discharged from the rear end of the threshing device. The threshing loss rate is calculated using the following formula:

$$Y_1 = \frac{M_1}{M} \times 100\% \quad (1)$$

Where: Y_1 – threshing loss rate, %; M_1 – mass of rapeseed collected in the material box at the rear end of the threshing device, g; M – total mass of rapeseed fed into the threshing device, g.

(2) Proportion of Threshed Material on the Sieve Surface

In the EDEM post-processing, a calculation region with a Grid Bin Group of 1×1×1 is established below the concave sieve to measure the mass of threshed material separated from the concave sieve-that is, the mass of threshed material falling onto the cleaning sieve surface. The proportion of residues on the sieve surface is calculated using the following formula:

$$Y_2 = \frac{M_2}{M_3} \times 100\% \quad (2)$$

where: Y_2 – proportion of threshed material on the sieve surface; M_2 – mass of threshed material in the material box below the concave sieve, g; M_3 – total mass of material fed into the threshing device, g.

(3) Left–right Distribution Ratio of Threshed Material on the Sieve Surface

In the EDEM post-processing, two collection regions with Grid Bin Groups of 2×1×1 are established on the left and right sides below the concave sieve to measure the weight of threshed material separated by the concave sieve on the left and right sides of the cleaning sieve surface.

The left–right distribution ratio of threshed material on the sieve surface is calculated using the following formula:

$$Y_3 = \frac{M_4}{M_5} \times 100\% \quad (3)$$

where:

Y_3 – left–right distribution ratio of threshed material on the sieve surface; M_4 – mass of threshed material in the right region of the sieve surface, g; M_5 – mass of threshed material in the left region of the sieve surface, g.

SIMULATION MODEL VALIDATION

A 3D model of the full-perimeter concave separation threshing device was established with a straw guide plate angle of 76° and a threshing gap of 7 mm. In the discrete element simulation model, the threshing drum speed was set to 650 rpm, and the reverse rotation speed of the concave sieve was set to 40 rpm, rotating in the opposite direction to the threshing drum. A tracked-type rapeseed combine harvester was used for preliminary testing, with overall dimensions (L × W × H) of 5120 × 2520 × 2720 mm and an engine power of 73 kW. According to preliminary field tests, the mass proportions of grains, pods, and short stalks in the threshed material were set as 25%, 30%, and 45%, respectively. The grain seed generation rate was set at 0.375 kg/s, the pod generation rate was set at 0.45 kg/s, and the short stalk stem generation rate was set at 0.675 kg/s, resulting in a total feed rate of 1.5 kg/s. The mass of lost rapeseed during threshing and the mass of the threshed material on the sieve surface obtained through simulation were 3.08144 g and 2215.94 g, respectively. Using the evaluation methods for the threshing device, the calculated loss rate of threshing entrainment was 0.27%, the proportion of threshed material residues on the sieve surface was 49.24%, and the left–right distribution ratio of threshed material residues on the sieve surface was 0.82.

To verify the accuracy of the simulation model, a field test device was designed and fabricated based on the structural dimensions of the designed full-perimeter rapeseed separation threshing device, as shown in Figure 4.

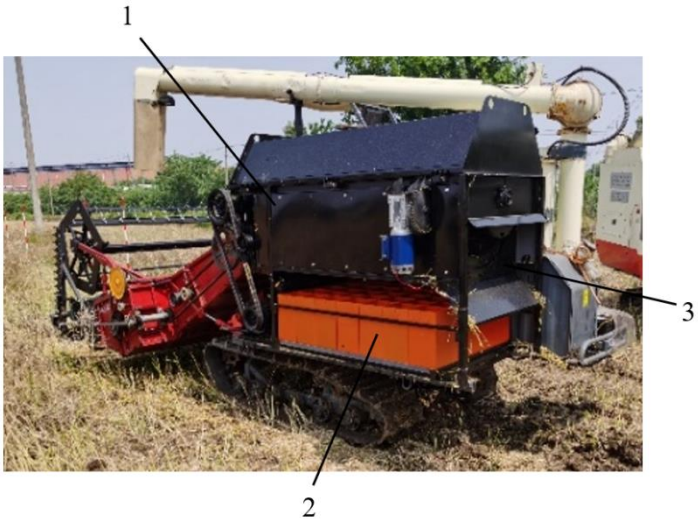

Fig. 4 - Test Platform of the Rapeseed Single Axial-Flow Full-Perimeter Separation Threshing Device
1. Threshing Drum Exit; 2. Sample Collection Box; 3. Separation and Cleaning Outlet

On May 24, 2024, a field experiment was conducted in Shiyezhou Town, Dantu District, Zhenjiang City, Jiangsu Province, to investigate threshing loss, the proportion of threshed material on the sieve surface, and the left–right distribution ratio of threshed material on the sieve surface. The test device operated with a cylinder rotation speed of 650 r/min, concave screen rotation speed of 40 r/min, a straw guide plate angle of 76°, and a threshing gap of 7 mm. The rapeseed variety used was Qin You 10, with grain moisture content at 24.2% and stalk moisture content at 65.7% during the test. The feeding rate was manually controlled at 1.5 kg/s. The field test results measured that the threshing loss rate was 0.60%, a proportion of threshed material on the sieve surface was 48.65%, and the left–right ratio of threshed material on the sieve surface was 0.84.

The absolute error of the threshing loss rate was 0.33%, and the relative error was 55%. The absolute errors of the proportion of threshed material on the sieve surface and the left–right distribution ratio of threshed material on the sieve surface were small, with relative errors of 1.21% and 2.38%, respectively. Compared with the field test results, the simulation analysis showed small absolute errors. Although the relative error for threshing loss was relatively larger, none of the errors exceeded an order of magnitude. Therefore, the established discrete element model of the rapeseed single axial-flow full-perimeter separation threshing device can be used for subsequent optimization of structural parameters.

EXPERIMENTAL DESIGN FOR PARAMETER OPTIMIZATION

Based on the established and validated discrete element model (DEM) of the single axial-flow full-perimeter separation threshing device for a rapeseed harvester, three key structural and operational parameters，namely threshing drum speed, straw guide plate angle, and threshing gap, were selected as

experimental factors. Multiple single-factor simulation analyses were conducted using three evaluation indicators: threshing loss rate, proportion of threshed material on the sieve surface, and the left–right distribution ratio of threshed material on the sieve surface.

Through a comprehensive assessment of the effects of each factor on the performance of the threshing device, the preliminary optimal ranges were determined as follows: threshing drum speed between 450 r/min and 650 r/min, straw guide plate angle between 74° and 78°, and threshing gap between 5 mm and 9 mm.

To further optimize the structural parameters of the single axial–flow full–perimeter separation threshing device for rapeseed, a three-factor, three-level Box-Behnken experimental design was employed to investigate the effects of threshing drum speed, straw guide plate angle, and threshing gap on the threshing loss rate, proportion of threshed material on the sieve surface, and the left–right distribution ratio of threshed material on the sieve surface. A comprehensive evaluation method was used to select the optimal parameter combination. The levels of the experimental factors are shown in Table 3.

Table 3

Levels of Factors in the Three-Factor, Three-Level Box-Behnken Experiment

Leve	Test Factors		
	Drum Speed *A* (r/min)	Straw Guide Plate Angle *B* (°)	Threshing Gap *C* (mm)
-1	450	74	5
0	550	76	7
1	650	78	9

RESULTS AND ANALYSIS

RESULTS AND ANALYSIS OF THE BOX-BEHNKEN EXPERIMENT

To analyze the significance of the effects of experimental factors on the evaluation indicators, the proportions of grains, siliques, and stalks generated in the particle factory during each simulation were randomly generated following a normal distribution to ensure the randomness and independence of the simulation test conditions.

The simulation duration was set to 3 seconds, and the material parameters for the simulation tests were configured according to the calibrated model parameters. The results of the three-factor, three-level Box-Behnken experiment are shown in Table 4.

Table 4

Results of the Three-Factor, Three-Level Box-Behnken Experiment

Test No.	Test Factors and Levels			Test Indicators		
	A (r/min)	*B* (°)	*C* (mm)	Y_1 (%)	Y_2 (%)	Y_3
1	450	76	5	0.32	47.54	0.80
2	450	74	7	0.37	45.79	0.90
3	450	78	7	0.33	48.42	0.84
4	450	76	9	0.36	44.78	0.86
5	550	74	5	0.32	47.39	0.92
6	550	78	5	0.27	49.86	0.77
7	550	76	7	0.29	47.17	0.88
8	550	76	7	0.29	46.97	0.88
9	550	76	7	0.29	47.07	0.87
10	550	76	7	0.29	47.07	0.87
11	550	76	7	0.30	47.07	0.88
12	550	74	9	0.34	45.83	0.93
13	550	78	9	0.31	47.12	0.83
14	650	76	5	0.25	49.54	0.80
15	650	74	7	0.28	48.82	0.92
16	650	78	7	0.25	50.55	0.75
17	650	76	9	0.27	48.14	0.82

The experimental results were analyzed using the Box-Behnken module in Design Expert 13. The analysis of variance (ANOVA) results for threshing loss rate, proportion of threshed material on the sieve surface, and the left–right distribution ratio of threshed material on the sieve surface discharge are shown in Tables 5, 6, and 7, respectively.

Table 5

Analysis of Variance for Threshing Loss Rate

Source	df	SS	MS	*F-value*	*P-value*
Model	9	0.0193	0.0021	143.27	< 0.0001
A	1	0.0136	0.0136	907.50	< 0.0001
B	1	0.0028	0.0028	187.50	< 0.0001
C	1	0.0018	0.0018	120.00	< 0.0001
AB	1	0.00001	0.00001	1.67	0.2377
AC	1	0.0001	0.0001	6.67	0.0364
BC	1	0.0001	0.0001	6.67	0.0364
A^2	1	0.0000	0.0000	2.12	0.1885
B^2	1	0.0007	0.0007	45.63	0.0003
C^2	1	0.0001	0.0001	7.74	0.0272
Residual	7	0.0001	0.0000		
Lack of Fit	3	0.0000	0.000008333	0.4167	0.751
Pure Error	4	0.0001	0.00001		
Total	16	0.0194			
R^2	0.9946				

Note: $p < 0.01$ indicates a highly significant effect; $0.01 < p < 0.05$ indicates a significant effect; $p > 0.05$ indicates no significant effect. Same below.

Table 6

Analysis of Variance for Proportion of Threshed Material from the Sieve Surface

Source	df	SS	MS	*F-value*	*P-value*
Model	9	36.02	4.00	386.66	< 0.0001
A	1	13.83	13.83	1336.60	< 0.0001
B	1	8.24	8.24	796.31	< 0.0001
C	1	8.95	8.95	864.39	< 0.0001
AB	1	0.2025	0.2025	19.57	0.0031
AC	1	0.4624	0.4624	44.68	0.0003
BC	1	0.3481	0.3481	33.63	0.0007
A^2	1	1.71	1.71	165.33	< 0.0001
B^2	1	1.99	1.99	192.28	< 0.0001
C^2	1	0.1813	0.1813	17.52	0.0041
Residual	7	0.0725	0.0104		
Lack of Fit	3	0.0525	0.0175	3.50	0.129
Pure Error	4	0.0200	0.0050		
Total	16	36.09			
R^2	0.998				

Table 7

Analysis of Variance for Left–right Distribution Ratio of Threshed Material on the Sieve Surface

Source	df	SS	MS	*F-value*	*P-value*
Model	9	0.0445	0.0049	117.37	< 0.0001
A	1	0.0015	0.0015	35.89	0.0005
B	1	0.0288	0.0288	683.39	< 0.0001
C	1	0.0028	0.0028	66.74	< 0.0001
AB	1	0.0030	0.0030	71.78	< 0.0001
AC	1	0.0004	0.0004	9.49	0.0178
BC	1	0.0006	0.0006	14.83	0.0063
A^2	1	0.0046	0.0046	108.80	< 0.0001
B^2	1	0.0004	0.0004	9.02	0.0199
C^2	1	0.0022	0.0022	52.85	0.0002
Residual	7	0.0003	0.00004		

Lack of Fit	3	0.0002	0.0001	1.94	0.2643
Pure Error	4	0.0001	0.00003		
Total	16	0.0448			
R^2	0.9934				

According to the ANOVA results in Tables 5, 6, and 7, the p-values for the models of threshing loss rate, proportion of threshed material on the sieve surface, and the left–right distribution ratio of threshed material on the sieve surface are all less than 0.0001, which is far below the conventional significance level of 0.05. This indicates that the assumed linear relationships in the models are reasonable. The coefficient of determination (R^2) for the threshing loss rate model is 0.9946, for the proportion of threshed material on the sieve surface is 0.998, and for the left–right distribution ratio of threshed material on the sieve surface is 0.9934, indicating that the regression models have a good fit. Regression equations describing the relationships between threshing loss rate, proportion of threshed material on the sieve surface, and left–right distribution ratio of threshed material on the sieve surface and the drum speed, straw guide plate angle, and threshing gap were obtained using Design Expert 13 software.

The regression equation for the threshing loss rate is shown in Equation (4).

$$R_1 = 21.57968 - 0.00149A - 0.50950B - 0.09213C - 0.00003AC + 0.00125BC + 0.00319B^2 + 0.00131C^2 \quad (4)$$

The regression equation for the proportion of threshed material on the sieve surface is shown in Equation (5).

$$R_2 = 934.74625 + 0.01663A - 24.4825B + 4.8675C - 0.00113AB + 0.0017AC - 0.07375BC + 0.00006A^2 + 0.17188B^2 - 0.05188C^2 \quad (5)$$

The regression equation for the left–right distribution ratio of threshed material on the sieve surface is shown in Equation (6).

$$R_3 = 11.3265 + 0.01429A - 0.33725B - 0.12013C - 0.00014AB - 0.00005AC + 0.00313BC - 0.00238B^2 - 0.00575C^2 \quad (6)$$

(1) ANALYSIS OF FACTORS AFFECTING THRESHING LOSS

The effects of drum speed, straw guide plate angle, and threshing gap on the threshing loss rate are shown in Figure 5. When the straw guide plate angle is at the central horizontal position (76°) and the drum speed is fixed, the threshing loss increases as the threshing gap becomes larger. When the threshing gap is fixed, the threshing loss decreases as the drum speed increases. When the drum speed is at the central horizontal position (550 r/min) and the threshing gap is fixed, the threshing loss increases as the straw guide plate angle becomes larger. When the straw guide plate angle is fixed, the threshing loss also increases with the increase of the threshing gap. After optimizing the parameters, the combination that minimizes threshing loss was obtained: drum speed of 648.675 r/min, straw guide plate angle of 77.860°, and threshing gap of 6.452 mm. At this point, the threshing loss rate is 0.246%.

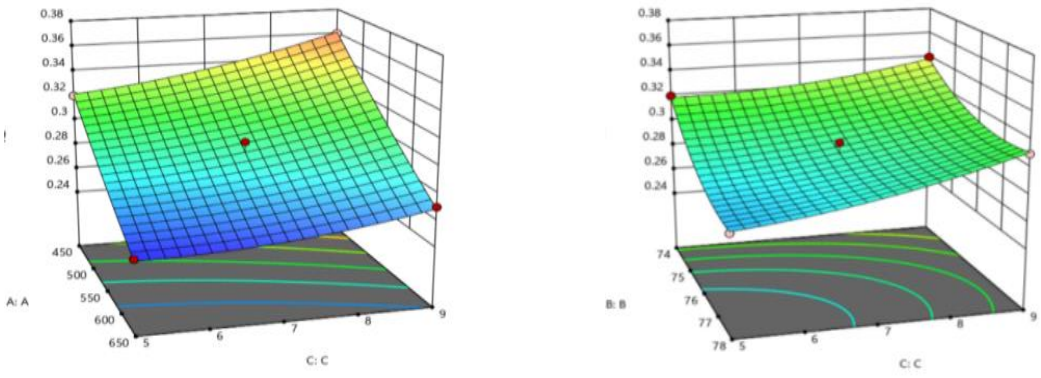

(a) Interaction Effect between Drum Speed and Threshing Gap

(b) Interaction Effect between Straw Guide Plate Angle and Threshing Gap

Fig. 5 - Effects of Drum Speed, Straw Guide Plate Angle, and Threshing Gap on Threshing Loss Rate

(2) ANALYSIS OF FACTORS AFFECTING THE PROPORTION OF THRESHED MATERIAL ON THE SIEVE SURFACE

The effects of drum speed, straw guide plate angle, and threshing gap on the proportion of material passing through the sieve surface are shown in Figure 6. When the threshing gap is at the central level (7 mm) and the drum speed is fixed, the proportion of material passing through the sieve decreases as the straw guide plate angle increases. When the straw guide plate angle is fixed, the proportion of material passing through the sieve increases with the increase in the drum speed. When the straw guide plate angle is at the central level (76°) and the drum speed is fixed, the proportion of material passing through the sieve decreases as the threshing gap becomes larger. When the threshing gap is fixed, the proportion of material passing through the sieve increases as the drum speed increases. When the drum speed is at the central level (550 r/min) and the threshing gap is fixed, the proportion of material passing through the sieve increases as the straw guide plate angle becomes larger. When the straw guide plate angle is fixed, the proportion of material passing through the sieve decreases as the threshing gap increases. After optimizing the parameters, the combination that minimizes the proportion of material passing through the sieve was obtained: drum speed of 461.41 r/min, straw guide plate angle of 74.090°, and threshing gap of 8.794 mm. At this point, the proportion of material passing through the sieve is 44.74%.

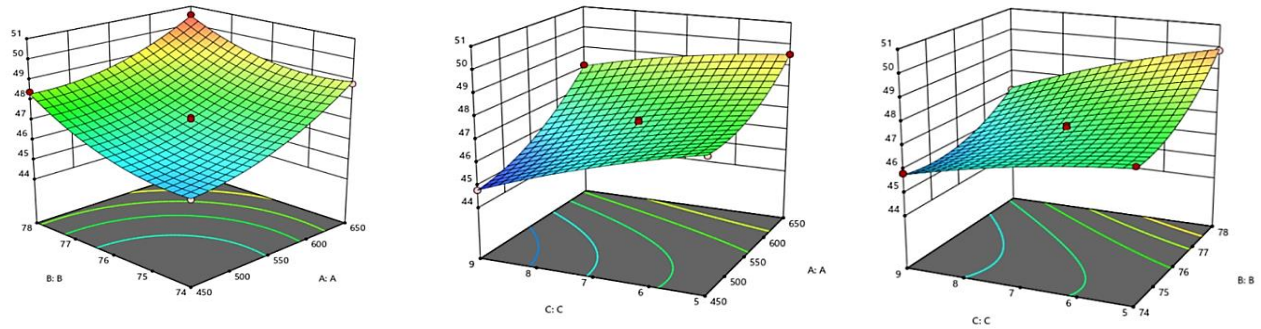

(a) Interaction Effect between Drum Speed and Straw Guide Plate Angle *(b) Interaction Effect between Drum Speed and Threshing Gap* *(c) Interaction Effect between Straw Guide Plate Angle and Threshing Gap*

Fig. 6 - Effects of Drum Speed, Straw Guide Plate Angle, and Threshing Gap on the Proportion of Material Passing Through the Sieve Surface

(3) ANALYSIS OF FACTORS AFFECTING THE LEFT–RIGHT DISTRIBUTION RATIO OF THRESHED MATERIAL ON THE SIEVE SURFACE

The effects of drum speed, straw guide plate angle, and threshing gap on the left–right distribution ratio of threshed material on the sieve surface are shown in Figure 7. When the threshing gap is at the central level (7 mm) and the drum speed is fixed, the left–right distribution ratio of threshed material on the sieve surface increases as the straw guide plate angle becomes larger, indicating a more uniform distribution of material across the sieve surface. When the straw guide plate angle is fixed, the uniformity of the left–right material distribution first improves and then deteriorates as the drum speed increases. When the straw guide plate angle is at the central level (76°) and the drum speed is fixed, the left–right distribution ratio of threshed material on the sieve surface initially increases and then decreases as the threshing gap becomes larger, indicating that the uniformity of material distribution across the sieve surface first improves and then declines. When the threshing gap is fixed, the uniformity of left–right material distribution first increases and then decreases as the drum speed increases. When the drum speed is at the central level (550 r/min) and the threshing gap is fixed, the left–right distribution ratio of threshed material on the sieve surface increases as the straw guide plate angle becomes larger. When the straw guide plate angle is fixed, the uniformity of the left–right material distribution first increases and then decreases as the threshing gap increases. After optimizing the parameters, the combination that maximizes the left–right distribution ratio of threshed material on the sieve surface was found to be: drum speed of 558.197 r/min, straw guide plate angle of 74.296°, and threshing gap of 7.195 mm. At this point, the left–right distribution ratio of threshed material on the sieve surface is 0.935.

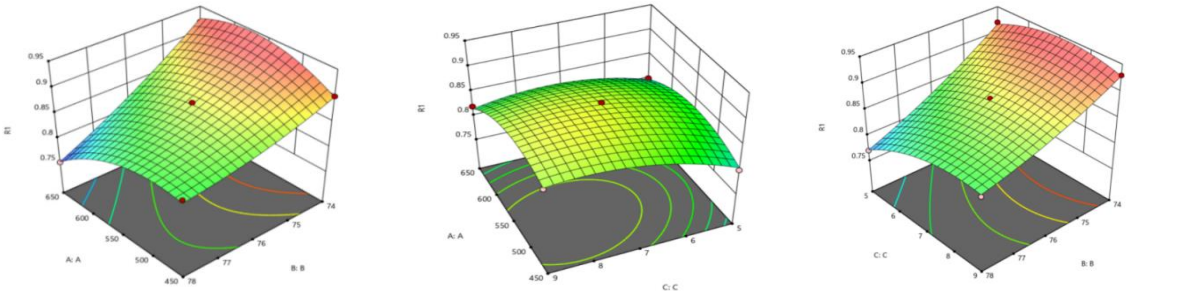

(a) Interaction Effect between Drum Speed and Straw Guide Plate Angle

(b) Interaction Effect between Drum Speed and Threshing Gap

(c) Interaction Effect between Straw Guide Plate Angle and Threshing Gap

Fig. 7 - Effects of Drum Speed, Straw Guide Plate Angle, and Threshing Gap on the Left–right Distribution Ratio of Material Passing Through the Sieve Surface

PARAMETER OPTIMIZATION

The interactions among drum speed, straw guide plate angle, and threshing gap in the single longitudinal axial flow full-periphery separation threshing device of the rapeseed harvester have different effects on threshing loss, the proportion of threshed material on the sieve surface, and the left–right distribution ratio of threshed material on the sieve surface. Under the conditions of minimal threshing loss, the proportion of threshed material on the sieve surface is minimized, and a larger left–right distribution ratio of threshed material on the sieve surface can improve the handling capacity and cleaning efficiency of the sieve surface material. Therefore, it is necessary to further optimize the relevant structure and operating parameters of the threshing device to achieve a comprehensive improvement. To identify the optimal solutions for the relevant factors, regression models relating threshing loss rate, proportion of threshed material on the sieve surface, and the left–right distribution ratio of threshed material on the sieve surface, and drum speed, straw guide plate angle, and threshing gap were established as objective functions. The solved parameter ranges were used as constraints, and the optimal solutions of the objective functions were obtained using Design Expert software. The optimization objectives and constraints are shown in Equation (7).

$$\begin{cases} \min\ Y_1 Y_2(A,B,C), \max\ Y_3(A,B,C) \\ s.t. \begin{cases} 450r/\min \le A \le 650r/\min \\ 74^\circ \le B \le 78^\circ \\ 5mm \le C \le 9mm \end{cases} \end{cases} \tag{7}$$

The optimal operating parameters were determined as follows: drum speed of 576.479 r/min, straw guide plate angle of 74.797°, and threshing gap of 7.687 mm. Under these conditions, the threshing loss rate was 0.301%, the proportion of threshed material on the sieve surface was 46.841%, and the left–right distribution ratio of threshed material on the sieve surface was 0.914. Considering the actual working conditions and processing requirements of the combine harvester, the optimized parameter set was adjusted to: drum speed of 550 r/min, straw guide plate angle of 75°, and threshing gap of 8 mm.

FIELD TEST EVALUATION

Based on the chassis, cutter bar, and cleaning system of the Xingguang 4LZY-4.0Z rapeseed combine harvester, the single longitudinal axial flow full-periphery separation threshing device designed in this study was installed. The main structure and technical parameters of the Xingguang 4LZY-4.0Z rapeseed combine harvester are shown in Table 8.

Table 8

Main Structure and Technical Parameters of the 4LZY-4.0Z Rapeseed Combine Harvester

Parameter	Value
Overall Dimensions (L × W × H) / （mm×mm×mm）	5190×2640×2980
Structural Type	Full-Feeding Crawler Self-Propelled Type
Engine Power (kW)	73.5
Rated Engine Speed (r·min^{-1})	2400
Working Cutting Width (m)	2.1
Feeding Rate (kg·s^{-1})	0–4
Operating Speed (km·h^{-1})	0–5.69

On May 29, 2025, in Shiyezhou Town, Dantu District, Zhenjiang City, Jiangsu Province, a third-party testing agency, Zhejiang Electromechanical Product Quality Institute Co., Ltd., was commissioned to conduct performance tests. The tests were carried out in accordance with the Chinese national standards GB/T 8097-2008 “Harvesting Machinery – Combine Harvester Test Methods” and DG/T 057-2019 “Rapeseed Harvester,” as well as agricultural machinery appraisal procedures. The field performance test setup is shown in Figure 8, and the testing conditions are listed in Table 9. According to the third-party performance test, the total loss rate was 5.6%, impurity rate 2.3%, and breakage rate 0.4%, with an operational hourly productivity of 0.57 hm²/h. These performance indicators exceed the requirements specified in NY/T 2199-2012 “Quality Standards for Rapeseed Combine Harvester Operations”.

Fig. 8 - Field Performance Test of the Rapeseed Single Longitudinal Axial Flow Full-Periphery Separation Harvester

Table 9

Field Test Conditions

Test Items	Unit	Test Result
Weather	/	Overcast
Temperature	℃	19.9–23.3
Humidity	RH/%	59.4–62.7
Test Field (Length × Width)	m	70×30
Slope and Ground Conditions	/	Flat Terrain
Crop Variety	/	Yueyou 1510
Maturity Stage	/	Fully Mature Stage
Natural Height	mm	1712
Lowest Pod Height	mm	650
Root Diameter	mm	10
Canopy Diameter	mm	600
Grain Moisture Content	%	15.1
Operating Speed	km/h	2.93
Working Width	mm	2100

DISCUSSION

The threshing device is the core working component of the rapeseed harvester. Optimizing the performance of the threshing device solely by evaluating threshing loss is insufficient. In the extreme case where all the material entering the threshing system is completely crushed and separated by concave screens to fall onto the cleaning sieves, the threshing loss would be zero. However, on the one hand, a large amount of threshed material then falls onto the cleaning sieves, which leads to excessive material load on the sieve surface. This results in untimely cleaning and increased cleaning losses, thereby adversely affecting the overall harvesting loss. On the other hand, if the threshed material are unevenly distributed on the cleaning sieve surface, local accumulation of threshed material in certain areas will make grain separation more difficult. Similarly, areas with fewer threshed material cannot fully utilize the separation capacity of the cleaning sieve. Therefore, optimizing the performance of the threshing device should not focus solely on the loss during the threshing stage. It is also necessary to comprehensively consider the proportion of threshed material and the distribution of threshed material on the sieve surface, which optimizes the performance of the threshing device through a multi-criteria approach.

The movement and forces acting on the material inside the threshing device during threshing are complex. Field experiments for optimization require high labor intensity and long testing periods. Additionally, the material properties of the crop vary significantly with the harvesting period, resulting in considerable errors when combining experimental data. This study attempts to use EDEM software to build a discrete element model (DEM) of rapeseed threshing and separation, establishing an evaluation and optimization model for the performance of the threshing device. The model was validated through comparison with field experiments.

The relative error in threshing loss was relatively large, while the relative errors in the proportion of threshed material on the sieve surface and the left–right distribution ratio of threshed material on the sieve surface were relatively small. This is mainly because grain separation and material carryover are affected by particle contact parameters and material distribution states, whereas the distribution of threshed material is less influenced by the intrinsic properties of the material. These findings also indicate that relying solely on simulation analysis to accurately evaluate threshing loss is challenging. This study conducted a simulation analysis of threshing loss by combining preliminary experiments with the composition of the threshing residues. The absolute error in the threshing loss rate was small, while the relative error was larger, though it did not exceed an order of magnitude. Therefore, it is still feasible to carry out parameter optimization based on the trend of changes in the threshing loss rate.

CONCLUSIONS

To optimize the performance of the single axial-flow full-perimeter separation threshing device of the rapeseed harvester, a comprehensive evaluation method was proposed using three indicators: threshing loss, proportion of threshed material on the sieve surface, and the left–right distribution ratio of threshed material on the sieve surface. A discrete element model (DEM) of rapeseed threshing and separation was established based on EDEM software. Comparison between simulation results and bench tests showed that the absolute error of threshing loss was 0.33%, with a relative error of 55%. The relative errors for the proportion of threshed material on the sieve surface and the left–right distribution ratio of threshed material were 1.21% and 2.38%, respectively. All errors between simulation and bench tests were within one order of magnitude, validating the feasibility of using the discrete element method to analyze and optimize the threshing device.

Using threshing drum speed, straw guide plate angle, and threshing gap as experimental factors, and threshing loss, proportion of threshed material on the sieve surface, and the left–right distribution ratio of threshed material on the sieve surface as evaluation indicators, a three-factor, three-level Box-Behnken experiment was conducted. Regression models were established between experimental factors and evaluation indicators. Through multi-objective optimization and considering the actual working conditions and processing requirements of the rapeseed combine harvester, the optimized parameter combination was determined as: drum speed of 550 r/min, straw guide plate angle of 75°, and threshing gap of 8 mm.

Under the optimal structure and operating parameters, a prototype was fabricated and entrusted to a third-party testing agency to evaluate the rapeseed harvesting operation. Field measurements showed a total harvesting loss rate of 5.6%, impurity rate of 2.3%, and grain breakage rate of 0.4%, with an operational productivity of 0.57 ha/h. The performance exceeded industry standard requirements, validating the feasibility and accuracy of the optimization method and results through field testing.

ACKNOWLEDGEMENT

This research was supported by National Key R&D Program of China (2023YFD2001000) and Funds for Modern Agricultural Industry Technology System Construction of China (CARS-12)

REFERENCES

[1] Dai F., Song X.F., Shi R.J., Guo W.J., Zhao Y.M., Wang F., Zhao W.Y. (2022). Movement law of the threshing material in threshing and cleaning machine for plot-bred wheat. *International Journal of Agricultural and Biological Engineering*,15(3), 100–106.

[2] Dong J. Q., Zhang D. X., Yang L., Cui T., Zhang K. L., He X. T., Wang Z. D., Jing M. S. (2023). Discrete element method optimization of threshing components to reduce maize kernel damage at high moisture content. *Biosystems Engineering*, 233, 221–240.

[3] Fang X.W., Zhang J.S., Zhao X.L., Zhang L., Zhou D.Y., Yu C.S., Hu W., Zhang Q. (2024). Optimising maize threshing by integrating DEM simulation and interpretive enhanced predictive modelling. *Biosystems Engineering*, 244, 93–106.

[4] Fu J., Zhang J.L., Liu F.S. (2024). Enhanced sieving mechanism of novel cleaning screen and investigation of particle movement characteristics on the screen. *Powder Technology*, 431, 119043.

[5] Jiang T., Li H.T., Guan Z.H., Mu S.L., Wu C.Y., Zhang M. (2023). Design and experiments of material uniform dispersion and diversion device on cleaning screen surface for oilseed harvesting. *Transactions of the Chinese Society for Agricultural Machinery*, 54(1), 164–176.

[6] Mirzazadeh Ali, Abdollahpour Shamsollah, Mahmoudi Asghar, Bukat A.R. (2012). Intelligent modeling of material separation in combine harvester's thresher by ANN. *International Journal of Agriculture and Crop Sciences*, 4(23), 1767–1777.

[7] Miu PI，Kutzbach HD. (2007). Mathematical model of material kinematics in an axial threshing unit[J]. *Computers and Electronics in Agriculture*, 58(2), 93–99.

[8] Qian Z.J., Jin C.Q., Zhang D.G. (2017). Multiple frictional impact dynamics of threshing process between flexible tooth and grain kernel. *Computers and Electronics in Agriculture*, 141, 276–285.

[9] Tang Z., Li Y. M., Wang C. H. (2013). Experiments on variable-mass threshing of rice in the tangential-longitudinal-flow combine harvester. *Journal of Agricultural Science and Technology*, 15(4), 1319–1334.

[10] Tang Z., Li Y.M., Xu L.Z., Pang J., Li H.C., (2012). Experimental study on wheat rate of tangential-axial combine harvester. *Transaction of the Chinese Society of Agricultural Engineering*, 28(5), 26–31.

[11] Teng Y.J., Jin C.Q., Chen Y.P., Liu P., Yin X., Wang T.E., Yu K. (2020). Design and optimization of segmented threshing device of combine harvester for rice and wheat. *Transactions of the Chinese Society of Agricultural Engineering*, 36(12), 1–12.

[12] Trollope J.R. (1982). A mathematical model of the threshing process in a conventional combine thresher. *Journal of Agricultural Engineering Research*, 27(2), 119–130.

[13] Wang Q.R., Mao H.P., Li Q.L. (2020). Modelling and simulation of the grain threshing drum for rice combine harvester using MBD-DEM coupling simulation. *Computers and Electronics in Agriculture*, 178, 106859.

[14] Wu Z., Chen J., Ma Z. (2024). Development of a lightweight online detection system for impurity content and broken rate in rice for combine harvesters. *Computers and Electronics in Agriculture*, 218:18689.

[15] Xu L.Z., Li Y.M. (2011). Modeling and experiment to threshing unit of stripper combine. *African Journal of Biotechnology*, 10(20), 4106–4113.

[16] Xu L.Z., Li Y.M., Chai X.Y. (2020). Numerical simulation of gas-solid two-phase flow to predict the cleaning performance of rice combine harvesters. *Biosystems Engineering*, 190, 11–24.

[17] Xu L.Z., Li Y.M., Wang C.H., Xue Z. (2014). A combinational threshing and separating unit of combine harvester with a transverse tangential cylinder and an axial rotor. *Transactions of the Chinese Society for Agricultural Machinery*, 45(02), 105–108,135.

[18] Yang F.F., Yan C.L. (2018). Movement analysis of cereal in axial flow threshing roller space. *Transactions of the Chinese Society for Agricultural Machinery*, 39(11), 48–50.

[19] Yang F.F., Yan C.L., Yang B.N., Yi S.J., Jiang N. (2010). Simulation and testing of cereal motion in threshing unit of combine harvester with axial feeding. *Transactions of the Chinese Society for Agricultural Machinery*, 41 (12), 67–81, 88.

[20] Yang L., Zhang X.L., Li Y.M., Lv L.Y., Shi M.L. (2024). Modeling and control methods of a multi-parameter system for threshing and cleaning in grain combine harvesters. *Computers and Electronics in Agriculture*, 225, 109251.

[21] Yuan L.H., He X., Zhu C.H, Wang W.Z., Wang M.L, Wu S.J. (2024). Design and test of tangential and longitudinal-axial threshing and separating unit for wheat. *Microelectronics Journal*, 21, 101774.